Inhibition and Gap Junction Effects on Synchronization Enhancement in Bushy Cells of Ventral Cochlear Nucleus

Melih Yayli, Ian C. Bruce

Department of Electrical & Computer Engineering, McMaster University, Hamilton, ON, Canada

Abstract

Auditory nerve fibers (ANFs) show synchronized firing behavior to low-frequency input stimuli. This kind of behavior is even more prominent in bushy cells of ventral cochlear nucleus (VCN) (Joris and Smith, 2008; Joris et al., 1994). Synchrony enhancement in globular bushy cells (GBCs), which receive synaptic inputs from many ANFs, can be explained by a coincidence detection mechanism performed by these cells. However, the possible mechanisms behind spherical bushy cell (SBC) synchrony enhancement are still unclear, since they receive very few excitatory inputs from ANFs. Gómez-Nieto and Rubio (2009, 2011) showed that the bushy cells of VCN are also connected to each other somatically via structures called gap junctions.
In this study, bio-physically detailed neural network models of globular and spherical bushy cell microcircuits of VCN are created based on the approach of Manis and Campagnola (2018). Temperature scaling and alternative sodium channel models are also included in the model implementation. The model takes its excitatory inputs from phenomenological ANF model of Bruce et al. (2018). The effects of broadband and narrowly tuned inhibition (coming from D-stellate cells and tuberculoventral cells respectively) on synchronization are inspected. Different gap junction levels presented in the model and their effect on synchronization are also examined.
Preliminary results suggest that, while inhibition and gap junctions can affect the synchronization of model spherical bushy cells to low-frequency tones, they cannot fully explain the degree of synchronization and entertainment exhibited by the published data.

I. INTRODUCTION

ANFs demonstrate synchronous firing to low frequency sinusoidal stimuli. This behaviour can be quantized by the Synchronization Index (SI), which is obtained from the period histogram. SI values range from 0 (flat period histogram) to 1 (only one bin containing all the spikes). The synchronous firing behaviour of ANFs depends on factors such as spontaneous rate (SR), characteristic frequency (CF), and the frequency and sound pressure level (SPL) of the stimulus.
Several studies have inspected the synchronous firing behaviour in ANFs and VCN bushy cells. Studies such as Joris et al. (1994), Joris and Smith (2008) and Spirou et al. (2005) indicate that the synchronous firing behaviour seen in ANFs is enhanced in the SBCs and GBCs. As an example, the SI vs SPL plots and raster plots in Fig. 1 show the enhancement in the synchronous firing pattern of BS cells, as measured at their axons in the trapezoid body (TB).

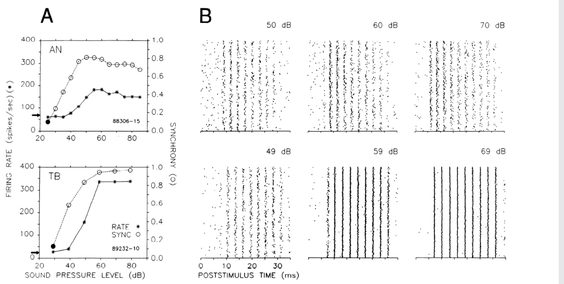

Figure 1: Comparison of ANF (top row) and BC (bottom row) cells' SI scores and firing rates across different SPL. Raster plots are good visualization tools in terms of showing the synchronous firing of ANF and bushy cells. Each dot represents a spike in the specific time bin.

SBCs and GBCs receive excitatory and inhibitory inputs via chemical and electrical synapses (also known as gap junctions). Fig. 2 shows an illustration of a bushy cell network with various type of connections. Transmission via the chemical synapse relies on release of the neurotransmitters to the synaptic cleft and their binding on the receptor proteins of the post-synaptic neuron, causing a post-synaptic potential (PSP). On the other hand, transmission via gap junction is more direct. The pre- and post synaptic membranes are physically close with each other and connected via channel proteins. These openings create a bidirectional link between the intracellular potentials of the connected neurons. Gap junctions are suggested to play a crucial role in the synchronization between neurons (Fukuda and Kosaka, 2000; Saraga et al., 2006).

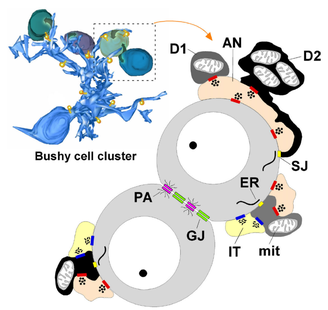

Figure 2: Top left: A 3D reconstruction of a VCN bushy cell cluster. Bottom right: Various connections between four bushy cells in the cluster. The soma-somatic connections are characterized as puncta adherentia (PA) and gap junctions (GJ). Other abbrevations are as follows: AN, auditory nerve; CB, cell body; D1, dendrite 1; D2, dendrite 2; ER, endoplasmic reticulum; IT, inhibitory terminal; SJ, sarcoplasmic junctions; mit, mitochondria. From Gómez-Nieto and Rubio (2009).

II. METHODS

- Figure 3 shows the network structure constructed for this study. The network consists of 4 layers: Auditory Nerve Fibers, D-Stellate Cell Layer, Tuberculoventral Cell Layer and Bushy Cell Layer. To explore the effect of gap junction on bushy cells, they are connected with each other via I_{gap1} and I_{gap2} in their respective membrane equations:

$$C_m\frac{dV_1}{dt} = -(I_{HT1} + I_{LT1} + I_{Na1} + I_{A1} + I_{h1} + I_{lk1} + I_{syn1} + I_{gap1} - I_{ext1}) \quad (1)$$

$$C_m\frac{dV_2}{dt} = -(I_{HT2} + I_{LT2} + I_{Na2} + I_{A2} + I_{h2} + I_{lk2} + I_{syn2} + I_{gap2} - I_{ext2}) \quad (2)$$

where I_{HT} is the high-threshold K^+ current, I_{LT} is the low-threshold K^+ current, I_{Na} is the fast Na^+ current, I_A is the fast inactivating current, I_h is the hyperpolarization-activated cation current, I_{lk} is the leakage current. The excitatory and inhibitory synaptic currents are modelled as I_{syn}. The cell models can take current injections via I_{ext}. I_{gap1} and I_{gap2} are defined as:

$$I_{gap1} = g_{gap}(V_1 - V_2); \quad (3)$$

$$I_{gap2} = g_{gap}(V_2 - V_1); \quad (4)$$

I_{gap1} and I_{gap2} allows the changes in the cells membrane voltages effecting each other directly (Figure 4).
Parameters and detailed current mechanisms to create cell structures and specific connectivity parameters that defines the connections between cells can be found in the repository provided by Manis and Campagnola (2018); `http://www.github.com/cnmodel`.

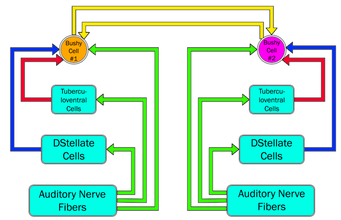

Figure 3: VCN bushy cell microcircuit structure used in this study. Green lines represent the excitatory inputs originating from ANFs. Blue lines represent inhibitory inputs from DStellate cells while red lines represent inhibitory inputs from Tuberculoventral cells. Yellow lines represent the gap junction connections between the bushy cells. Bushy Cell 1 has a characteristic frequency of 340Hz while the Bushy Cell 2 has a CF of 400Hz.

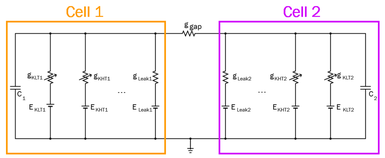

Figure 4: A circuit model representation of two cells connected via gap junctions.

- The SI calculations are performed according to Joris et al. (1994). A 350 Hz pure tone stimulus is applied repeatedly for 25 ms followed by a 75 ms silent period for a total recording duration of 20 seconds.
- Spherical bushy cells receive excitatory inputs from 3 high spontaneous rate (HSR) ANFs and globular bushy cells receive 12 HSR ANF inputs. While 7 DStellate and 6 Tuberculoventral cells provide inhibitory inputs to both cell types. DStellate cells receive broadband excitation from a mix of 36 low, medium and high spontaneous rate ANFs. Tuberculoventral cells receive excitatory inputs from 24 low and medium spontaneous rate ANFs. The convergence parameters provided in Table 1 indicate how much of spread these excitatory inputs have in frequency. The synaptic convergence and range parameters are introduced in Tables 1 and 2, respectively.

Table 1: Synaptic Convergence Parameters (number of cells)

	Model Type					
	bushy	tstellate	dstellate	octopus	pyramidal	tuberculoventral
ANF	3.3	6.5	35	60	48	24
dstellate	7	20	3	0	15	15
tstellate	0	0	0	0	0	0
tuberculoventral	6	6	0	0	21	0
pyramidal	0	0	0	0	0	0

Table 2: Synaptic Convergence Range Parameters (octaves)

	Model Type					
	bushy	tstellate	dstellate	octopus	pyramidal	tuberculoventral
ANF	0.05	0.1	0.4	0.5	0.1	0.1
dstellate	0.208	0.347	0.5	0	0.2	0.2
tstellate	0.1	0.1	0	0	0	0
tuberculoventral	0.069	0.111	0	0	0.15	0
pyramidal	0	0	0	0	0	0

- Different levels of inhibition are introduced by multiplying the combined inhibitory inputs coming from DStellate and Tuberculoventral cells with 0 (no inhibition), 0.5 (partial inhibition) and 1 (full inhibition). The gap junctions' effect on the firing rate and synchrony of the bushy cell is inspected by changing the g_{gap} to 0, 12.5nS, 25nS, 50nS and 125nS.

III. RESULTS

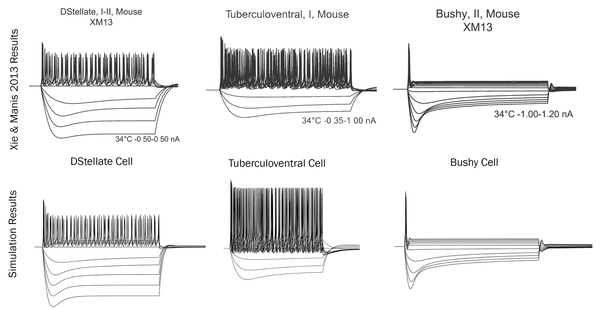

Figure 5: Top row: Xie and Manis (2013) type cell current injection results presented in Manis and Campagnola (2018). Bottom row: Current injection simulation results. The amount of injected currents are matched with the levels presented in Manis and Campagnola (2018).

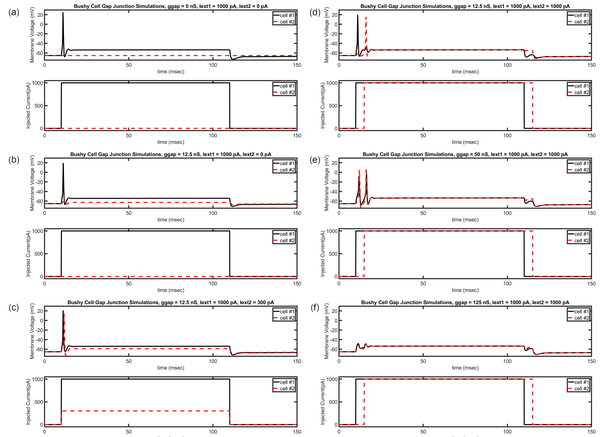

Figure 6: (a) Cells are not connected with a gap junction. When the first cell is injected with a suprathreshold input it creates an action potential, but the second cell remains inactive. (b) When weak gap junctions are included, even though the second cell is not stimulated with an injected current, the membrane potential is perturbed. (c) When the second cell is injected with a subthreshold input (which would not cause the cell to spike by itself) an action potential is created with the help of the gap junction connection. (d), (e) and (f) show how different levels of gap junctions affect the firing of the cells. When both of the cells are introduced to a suprathreshold input, both are able to fire with a moderate gap junction strength. When g_{gap} is increased to 50nS, both cells fire two action potentials, i.e., the action potentials spread from cell to cell (with a decreased spike amplitude). At 125nS, even though both cells are injected with suprathreshold inputs, both cells fail to create an action potential.

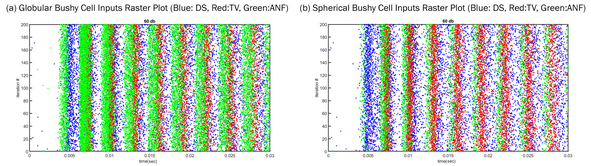

Figure 7: Raster plots of the excitatory and inhibitory inputs converging to (a) Spherical and (b) Globular Bushy cells at 60dbSPL. Raster plots of each ANF, DS and TV cells are placed on top of each other to give a better representation of the amount of excitation and inhibition that each bushy cell receives and the timing of these presynaptic occurings. Blue dots represent inhibitory inputs coming from DStellate cells while red dots indicate the instances of inhibition coming from Tuberculoventral cells. Green dots are excitation coming from auditory nerve fibers. Even though the SBC receives less excitation from ANF compared to the GBC, every instance of excitation is enough to cause an action potential (suprathreshold inputs), while the GBC needs a couple of subthreshold inputs occuring within a short time window to fire a spike (coincidence detection).

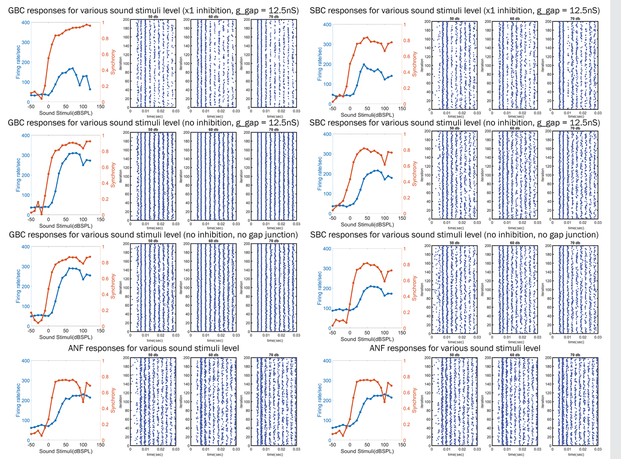

Figure 8: The plots on the left side of the raster plots shows the fire rate (blue) and SI scores (orange) of the SGCs and GBCs in different inhibition and gap junction conditions.

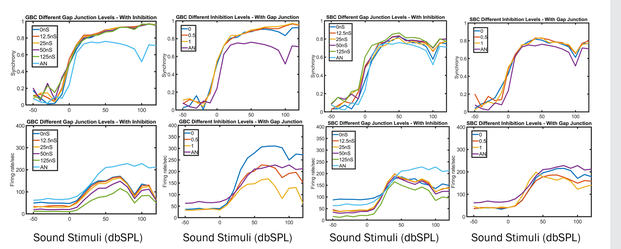

Figure 9: Changes in the fire rate and SI scores on various inhibition and gap junction levels. The four right hand plots show the synchrony (top row) and firing rate (bottom row) for GBC type cells. The four left hand plots show the same characteristics for the SBC type cells. While the decrease caused by inhibition in the fire rate was expected, initial results also indicate a consistent decrease on the fire rate with increasing gap junction conductance. While inhibition has a subtle effect on improving the SBC synchronization, the gap junctions effect on the synchrony seems to be stronger.

IV. CONCLUSIONS

- The inhibition coming from DS and TV cells appear to fill the gaps between syncronous firing patterns of ANFs. This might result in elimination of the spontaneous firing caused by ANFs and a narrower firing pattern for bushy cells.
- Initial results suggest that both the inhibition and the gap junctions have an effect on synchrony enhancement on SBCs. While there is a chance of this improvement being caused by the decrease in the firing rate, resulting in a narrower SBC firing patterns, more investigations with different inhibition and gap junction levels should be done.
- Preliminary results also suggests that neither inhibition nor gap junctions have a strong effect on the synchronization improvement in GBCs.

V. FUTURE WORK

- In this study only two bushy cells are connected to each other via gap junctions. A bigger network model including more bushy cells that are connected via gap junctions will be created to further investigate the gap junction's effect on firing patterns of the bushy cells.

REFERENCES

I. C. Bruce, Y. Erfani, and M. S. Zilany. A phenomenological model of the synapse between the inner hair cell and auditory nerve: Implications of limited neurotransmitter release sites. *Hearing Research*, 360:40–54, 2018.
T. Fukuda and T. Kosaka. The dual network of gabaergic interneurons linked by both chemical and electrical synapses: a possible infrastructure of the cerebral cortex. *Neuroscience research*, 38(2):123–130, 2000.
R. Gómez-Nieto and M. E. Rubio. A bushy cell network in the rat ventral cochlear nucleus. *Journal of Comparative Neurology*, 516(4):241–263, 2009.
R. Gómez-Nieto and M. E. Rubio. Ultrastructure, synaptic organization, and molecular components of bushy cell networks in the anteroventral cochlear nucleus of the rhesus monkey. *Neuroscience*, 179:188–207, 2011.
P. X. Joris and P. H. Smith. The volley theory and the spherical cell puzzle. *Neuroscience*, 154(1):65–76, 2008.
P. X. Joris, L. H. Carney, P. H. Smith, and T. Yin. Enhancement of neural synchronization in the anteroventral cochlear nucleus. i. responses to tones at the characteristic frequency. *Journal of Neurophysiology*, 71(3):1022–1036, 1994.
P. B. Manis and L. Campagnola. A biophysical modelling platform of the cochlear nucleus and other auditory circuits: from channels to networks. *Hearing Research*, 360: 76–91, 2018.
F. Saraga, L. Ng, and F. K. Skinner. Distal gap junctions and active dendrites can tune network dynamics. *Journal of neurophysiology*, 95(3):1669–1682, 2006.
G. Spirou, J. Rager, and P. Manis. Convergence of auditory-nerve fiber projections onto globular bushy cells. *Neuroscience*, 136(3):843–863, 2005.
R. Xie and P. B. Manis. Target-specific ipsc kinetics promote temporal processing in auditory parallel pathways. *Journal of Neuroscience*, 33(4):1598–1614, 2013.

yaylim@mcmaster.ca | ibruce@ieee.org

Supported by NSERC Discovery Grant #RGPIN-2018-05778.